Optical Asymmetric filter Using Graphene Plasmonic embedded in Photonic Crystal Fiber

Zainab Mohammed AL-Wahhamy[1], Muwafaq F. Jaddoa[2] and Firas Faeq K. Hussain[1,2,*]

[1] *Department of Physics, College of Science, Al-Muthanna University , Muthanna, Iraq*

[2] *College of Engineering, Al-Ayen Iraqi University, Dhi-Qar, Iraq.*

[*]*Corresponding Author:* muwafaq@mu.edu.iq

Received 10 Feb. 2025, Accepted 1 Mar. 2025, Published 30 June. 2025.

DOI: 10.52113/2/12.01.2025/13-21

Abstract: This work exhibits simulation and design of a small-scale graphene plasmonic filter based photonic crystal fiber through finite element method investigation. Some cladding holes inside the PCF possess deposited 2-D graphene enabling the light transmission interaction which leads to surface plasmonic resonance (SPR). Improved optical filter performance results from this process because it enables better control and higher sensitivity and reduced signal loss so filters become optimal for use. A finite element method analyzes both polarization properties and spectral loss performance in the proposed structural design. The simulation evaluation was divided into two testing periods while changing the dimensions of PCF geometry. The investigation of first design components incorporated r = 6 and r = 5 while the second design components incorporated r = 6 and r = 7. The introduction of graphene materials into PCF rings comprises the two design models progressively from one to four rings. The design suffered maximum loss when four graphene rings were inserted in both designs. The absorption increases results in the creation of plasmonic polaritons. In the first design, when r = 6 and r = 5, the quasi-TE guided mode exhibits losses of -113000 dB/ mm for wavelengths λ = 1.14 μm. The quasi-TM guided mode exhibits losses of -109100 dB/ mm for wavelengths λ = 1.17 μm . In the second design, r = 6 and r = 7, the losses of the quasi-TE guided mode are -146800 dB/ mm for wavelengths λ = 1.16 μm. The quasi-TM guided mode exhibits losses of -146600 dB/mm at wavelengths λ = 1.2 μm.

***Keywords*:** photonic crystal fiber, Graphene, surface plasmon polarization, polarization filters.

1. Introduction

Scientists can achieve essential property customization through photonic fibers by modifying their structure which enables optical applications in a wide range of applications [1].

Scientists can achieve essential property customization through photonic fibers by modifying their structure which enables

optical applications in a wide range of applications [1]. The fibers function as

selective light filters for polarized beams since such capabilities play a vital role in managing optical system behavior [3] [2]. These fibers show improved light transmission behavior because metal occupation affects the process according to polarization directions. Such performance advantages enable sensor and filtering applications. The metal surface encounter from light light induces free electron oscillations that create surface plasmon waves to boost the coupling of light and matter [3-6]. Surface plasmon polarization waves (SPP) function as the mechanism by which light causes propagation on metallic materials to trigger surface plasmon resonance (SPR) [7, 8]. The SPR phenomenon expresses itself most prominently in noble metals such as gold and silver because these metallic elements show great research stability [9-12]. Additionally surface plasmon behavior occurs in insulating materials and semiconductors despite their unique frequency requirements [13]. The optical characteristics of fibers receive beneficial enhancement from graphene because it improves interactions between light and controls polarization [14, 15]. Graphene becomes available as a coating material for optical fibers to change refractive index properties and enable surface plasmon polariton (SPP) modes to combine with the core fiber modes [16, 17]. The functionality of wavelength switching in polarizing filters becomes possible through this capability which also boosts performance metrics including extinction ratio from a compact device design [18]. The fast response capability permits quick adjustments to light properties when chemical potential changes occur because of activation methods [19]. The joining of SPP and PCF technology creates a high-performance polarizing filter that efficiently confines light energy at particular wavelengths to optimize application performance [20]. In the past few years, In 2021 [15], A hybrid silver-graphene coated pentagonal Photonic Crystal Fiber (PCF) has been proposed as the basis for the polarization filter. At typical optical communication wavelengths of 1.31 μm and 1.55 μm, the proposed Photonic Crystal Fiber (PCF) based filter efficiently suppresses the undesirable Y-polarization mode with significantly high signal loss and separates the desired X-polarization mode with little signal loss. Reaching

cross-talk values of 216.68 dB and 904.67 dB at the corresponding wavelengths, the 300 μm-long PCF exhibits significant isolation between the two polarization modes, highlighting its potential for sophisticated optical communication systems. Also,In 2023 [22], They proposed a new polarization mode filter based on a graphene and gold-coated D-shaped photonic crystal fiber. Through the manipulation of the chemical potential, this filter can be used for single, dual, or three wavelength filtering. With a short device length of 100 μm and an extinction ratio of over 25 dB over the wavelength range of 1.0~1.4 μm, this filter has potential for use in multi-parameter sensing, WDM communication systems, and polarization modulation.

In this work, the dispersion benefits of the proposed structure are examined through modeling of graphene-photonic crystal fibers (Gr-PCF) based on a basic design, with a focus on effective index computation and spectrum loss (L dB). We also consider the effects of structural parameters like the air hole radius (r) of the cladding and the hole pitch (Λ).

2. Design Consideration

A schematic cross-section of the suggested Gr-PCF-based polarization filters is presented in Figure 1.The design consists of four air-holed circular rings distributed inside a silica background. In shape (a), the radius of the gaps at the top is r = 0.6 μm and the radius of the gaps at the bottom is r = 0.5 μm, and in structure (b), the radius of the gaps at the top is r = 0.6 μm and the radius of the gaps at the bottom is r = 0.7 μm, while the slope (Λ) represents the distance between them. Graphene with a thickness of r = 0.1 μm and multiple rings was repeatedly added around the gaps in the shell. Four ready-made distributions of graphene rings—single, double, triple, quadruple, and change in design—were considered in this work.

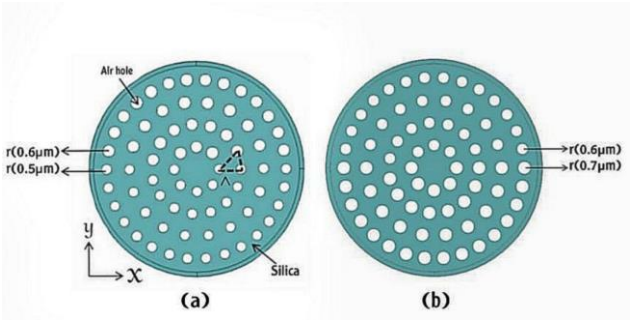

Fig. (1): Schematic cross-section of the proposed Gr-PCF based polarization filters (a) the first design r = 0.6 μm and r = 0.5 μm (b) the second design r = 0.6 μm and r = 0.7 μm .

Silica is used as the background material and its refractive index n (λ) is governed by Sellmeier equation [10]:

$$n(\lambda) = \sqrt{1 + \frac{0.6961663\lambda^2}{\lambda^2 - 0.0684043^2} + \frac{0.4079426\lambda^2}{\lambda^2 - 0.1162414^2} + \frac{0.8974794\lambda^2}{\lambda^2 - 9.86161^2}} \quad (1)$$

The permittivity (ε) of graphene is measured using the extended Drude model and defined as follows :

$$\varepsilon_{Gr} = 1 - i\frac{\sigma_{Gr}}{\omega\varepsilon_0 d_{Gr}} \quad (2)$$

Eq. (2) provides the permittivity of vacuum (ε_0) and the thickness of the graphene sheet (d_{Gr}). where $\omega = 2\pi c/\lambda$ is the angular frequency representation and i is the imaginary permittivity quantity.

3. Numerical Results

The characteristics of Gr-PCF were evaluated using a finite element technique solver, and the geometric parameters were tuned to guarantee strong mode confinement inside the SiO2 core. The first design parameters were set to a hole radius of r = 0.6 μm for the top, a hole radius of r = 0.5 μm for the bottom, and for the second design to a hole radius of r = 0.6 μm for the top, a hole radius of r = 0.7 μm for the bottom, and Λ = 2.5 μm. The research investigates the effects of air holes surrounded by a graphene layer on the properties of the proposed configuration. Variations in the number of rings are shown in Fig. 2.

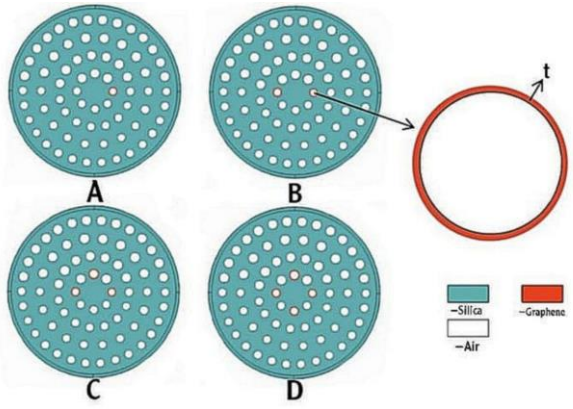

Fig. (2): Schematic structures of graphene rings placed in simplified Gr-PCF (a) single, (b) double, (c) triple, and (d) quadruple.

4. Modal Analysis of Gr-PCF

The number of typical graphene rings present in air holes determines both the structural behavior and fiber configuration. An increase in graphene rings leads to enhanced light absorption by the fiber which results in property changes for plasmonic polaritons. The frequency response of the polaritons modifies when light engages with numerous rings which increases performance of optical systems. The enhanced sensitivity of optical devices results from employing this technique which makes them better at detecting minimal signal variations. The study was conducted in four stages, the thickness of the graphene material fixed to 0.1 μm and in two parts, the first at gap radii r = 0.6 μm and r = 0.5 μm and the second part at r = 0.6 μm and r = 0.7 μm .The thickness of the graphene affects the amount of light it absorbs, which affects the efficiency of the filters. From Figure (3b), it is clear that at λ = 1.24 μm and λ = 1.74 μm, the losses are -12370 dB/ mm and -

6540 dB/mm for quasi-TE mode, while for quasi-TM mode the losses are -28760 dB/ mm and -13410 dB/ mm. In Figure (4b), it is clear that at λ = 1.22 µm and λ = 1.78µm, the losses are -14340 dB/ mm and -12010 dB/ mm for quasi-TE mode, while for quasi-TM mode the losses are -37930 dB/ mm and -77790 dB/ mm.

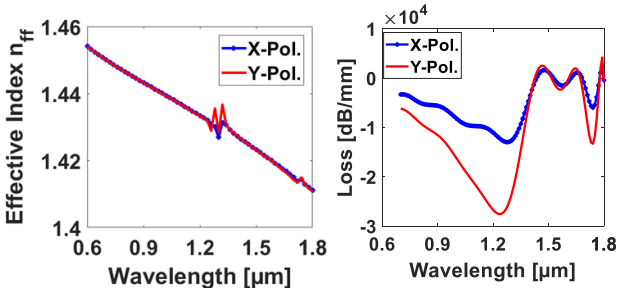

(a) (b)

Fig. (3): Effective wavelength (neff) and attenuation (dB/mm) dependence indices for the first design of Gr-PCF at gap radii r = 0.6 µm and r = 0.5 µm with a single graphene ring with thickness Gr = 0.1 µm.

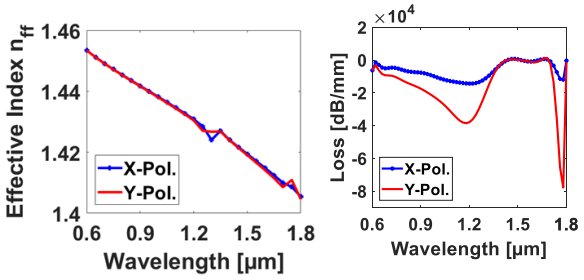

(a) (b)

Fig. (4): Effective wavelength (neff) and attenuation (dB/mm) dependence indices for the second design of Gr-PCF at gap radii r = 0.6 µm and r = 0.7 µm with a single graphene ring with thickness Gr = 0.1 µm.

In the second stage, by adding two rings that increase the light absorption capacity of graphene, the effective indices of guided modes and losses fluctuate with wavelength. Figure (5b) shows that the losses in the quasi-TM mode are -67840 dB/ mm for wavelength λ = 1.22 µm and those in the quasi-TE mode are -34080 dB/ mm for wavelength λ = 1.28 µm. From Figure (6b), it is clear that at λ = 1.2 µm and λ = 1.78µm, the losses are -34780 dB/ mm and -27020 dB/ mm for the quasi-TE mode, while for the quasi-TM mode the losses are -100300 dB/ mm and -178000 dB/ mm, respectively.

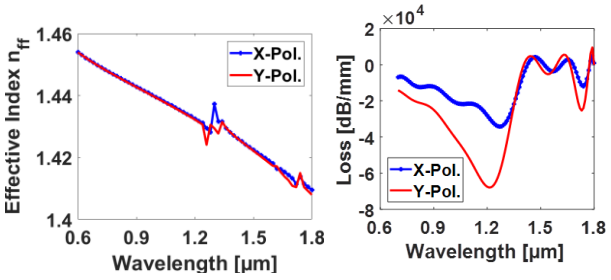

(a) (b)

Fig. (5): Effective wavelength (neff) and attenuation (dB/mm) dependence indices for the first design of Gr-PCF at gap radii r = 0.6 µm and r = 0.5 µm with two graphene rings of thickness Gr = 0.1 µm.

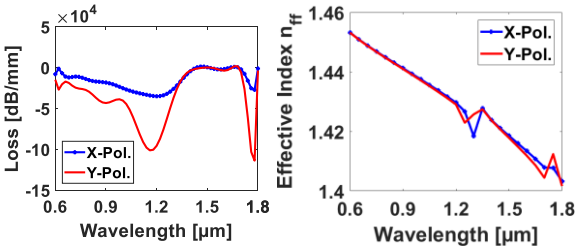

(a) (b)

Fig. (6): Effective wavelength (neff) and attenuation (dB/mm) dependence indices for the second design of Gr-

PCF at gap radii r = 0.6 μm and r = 0.7 μm with two graphene rings with thickness Gr = 0.1 μm.

Changing the number of graphene rings to three will change the interaction mechanism between light and graphene. This may lead to unexpected changes in the behaviour of light, resulting in sudden jumps in optical properties. As shown in Figure (4.20) and (4.21) it is clear from these images how the differences in contributors and other selections of causes vary according to the wave of poverty. The figure shows that the TM- and TE-guided modes exhibit remarkably sharp three wavelengths. It is observed that by increasing the number of graphene rings in the air holes, the connection between the fundamental modes and the super-SP modes can be enhanced.

As shown in Figure (4.20b), the losses of the quasi-TE guided mode are -57790 dB/ mm and -74200 dB/mm for wavelengths λ = 1.15 μm and λ = 1.74 μm, respectively. The quasi-TM guided mode exhibits losses of -80020 dB/ mm and -39620 dB/ mm for wavelengths λ = 1.18 μm and λ = 1.74 μm, respectively. These values indicate significant variations in losses, suggesting a complex interplay between the modes and the enhanced absorption characteristics of the graphene rings. As shown in Figure (4.21b) of the graph, the quasi-TE and quasi-TM modes exhibit two sharp jumps. The losses of the quasi-TE guided mode are -81240 dB/ mm and -59050 dB/ mm for wavelengths λ = 1.16 μm and λ = 1.78 μm, respectively. The quasi-TM guided mode exhibits losses of -119900 dB/ mm and -134900 dB/ mm at wavelengths λ = 1.2 μm and λ = 1.78 μm, respectively.

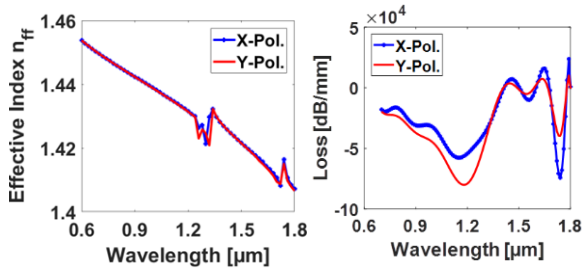

(a) (b)

Fig. (7): Effective wavelength (neff) and attenuation (dB/mm) dependence indices for the first design of Gr-PCF at gap radii r = 0.6 μm and r = 0.5 μm with three graphene rings with thickness Gr = 0.1 μm.

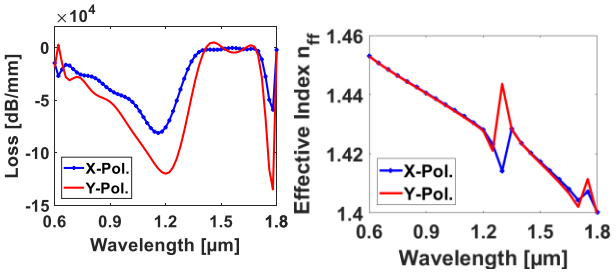

(a) (b)

Fig. (8): Effective wavelength (neff) and attenuation (dB/mm) dependence indices for the second design of Gr-PCF at gap radii r = 0.6 μm and r = 0.7 μm with three graphene rings with thickness Gr = 0.1 μm.

The last part of this work is where four graphene rings are added to study the polarization properties of the proposed Gr-PCF. This image

clearly shows that for the proposed Gr-PCF, almost all TE and TM modes will merge with the size of four graphene rings. This is because increasing the number of graphene rings leads to changes in the effective refractive index of the fiber. This modification can affect how different modes propagate in the fiber. When there is an overlap in the refractive index between the modes, it can lead to their merging. In Figure (4.22b) The quasi-TE guided mode exhibits losses of -113000 dB/ mm and -89650 dB/ µm for wavelengths λ = 1.14 µm and λ = 1.74 µm, respectively. The quasi- TM guided mode exhibits losses-109100 dB/ mm and -49640 dB/ µm for wavelengths λ = 1.17 µm and λ = 1.74 µm, respectively. As shown in Figure (4.23b) of the graph, the quasi-TE and quasi-TM modes exhibit two sharp jumps. The losses of the quasi-TE guided mode are -146800 dB/ mm and -130200 dB/ mm for wavelengths λ = 1.16 µm and λ = 1.78 µm, respectively. The quasi-TM guided mode exhibits losses of -146600 dB/mm and -155800 dB/mm at wavelengths λ = 1.2 µm and λ = 1.78 µm, respectively.

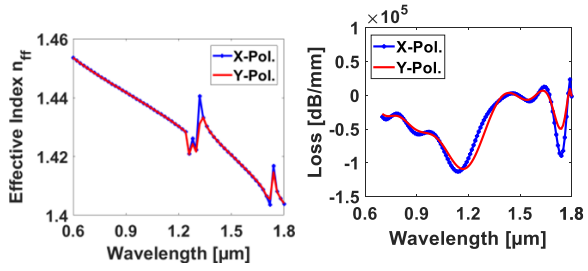

(a) (b)

Fig. (9): Effective wavelength (neff) and attenuation (dB/mm) dependence indices for the first design of Gr-PCF at gap radii r = 0.6 µm and r = 0.5 µm with four graphene rings with thickness Gr = 0.1 µm.

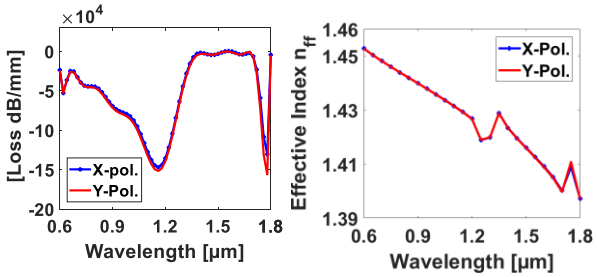

(a) (b)

Fig. (10): Effective wavelength (neff) and attenuation (dB/mm) dependence indices for the second design of Gr-PCF at gap radii r = 0.6 µm and r = 0.7 µm with four graphene rings with thickness Gr = 0.1 µm.

5. Conclusion

Analyze the impact of changes in graphene ring counts and design characteristics on photonic crystal fibers. The polarisation behaviour of Gr-PCF improves when graphene coats the airhole shell because it increases the interaction between surface plasmon (SP) supermodes and core-guided modes.The implementation of graphene within photonic crystal fibres (PCF) enables better optical filter performance by enabling precise control and improved sensitivity and decreased signal loss,oss thus making them suitable for various optical applications. The addition of rings leads to increased losses,osses while the gap dimension

determines how much loss occurs. More graphene rings enhance optical applications because these rings increase the amount of light absorption by the fiber. The quantity of rings in the design functions to increase the sensitivity of optical equipment,ipment which boosts their responsiveness to minimal signal variations. The filter's wavelength identification power depends on the structural elements of the fibre material. The processing range of frequencies through the fibre depends directly on its geometric design features together with its composed elements. This design stands unique from previous designs because it allows guided modes to interact with SP supermodes to transform coupling points at specific wavelengths. The proposed approach demonstrates excellent suitability for use in filtering devices.

References

[1] Chaudhary, Vijay Shanker, et al. "Advances in photonic crystal fiber-based sensor for detection of physical and biochemical parameters—A review." IEEE sensors journal 23.2 (2022): 1012-1023.

[2] AL-Kinani, Zahraa Ibrahim, and Firas Faeq K. Hussain. "Analysis of circular plasmonic photonic crystal fiber for filter applications." AIP Conference Proceedings. Vol. 2213. No. 1. AIP Publishing, 2020.

[3] Cao, Hui, et al. "Controlling light propagation in multimode fibers for imaging, spectroscopy, and beyond." Advances in Optics and Photonics 15.2 (2023): 524-612.

[4] Li, Tianshu, et al. "A refractive index sensor based on H-shaped photonic crystal fibers coated with Ag-graphene layers." Sensors 20.3 (2020): 741.

[5] Wang, Jianshuai, et al. "Wavelength-Switchable Polarization Filter Based on Graphene-Coated D-Shaped Photonic Crystal Fiber." Plasmonics 19.5 (2024): 2363-2370.

[6] Paul, Alok Kumar, et al. "Graphene/gold based photonic crystal fiber plasmonic temperature sensor for electric vehicle applications." 2019 22nd International Conference on Electrical Machines and Systems (ICEMS). IEEE, 2019.

[7] Kushwaha, Angad S., et al. "A study of improved bimetallic graphene–based fiber optic surface plasmon resonance (FOSPR) biosensor." Plasmonics 17.3 (2022): 1009-1016.

[8] Fu, Guangwei, et al. "A compact electro-absorption modulator based on graphene photonic crystal fiber." Chinese Physics B 29.3 (2020): 034209.

[9] Liu, Wei, et al. "A hollow dual-core PCF-SPR sensor with gold layers on the inner and

outer surfaces of the thin cladding." Results in Optics 1 (2020): 100004.

[10] Jing, Yiming, et al. "Polarization filter of hollow-core anti-resonant fiber in the 1550 nm band based on SPR effect." Optics & Laser Technology 180 (2025): 111407.

[11] Chen, Nan, et al. "Broadband plasmonic polarization filter based on photonic crystal fiber with dual-ring gold layer." Micromachines 11.5 (2020): 470.

[12] Qu, Yuwei, et al. "Mid-infrared silicon photonic crystal fiber polarization filter based on surface plasmon resonance effect." Optics Communications 463 (2020): 125387.

[13] Wang, Yue, et al. "Tunable all-fiber polarization filter based on graphene-assisted metal gratings for the O-and C-bands." Journal of the Optical Society of America B 40.11 (2023): 2868-2874.

[14] Dhameliya, Tejas M., et al. "Future of environment with carbon allotropes." Nirma University Journal of Pharmaceutical Sciences 11.1 (2024): 33-54.

[15] Lavanya, A., and G. Geetha. "Broadband polarization filter based on hybrid silver-graphene coated pentagonal photonic crystal fiber." Optical and Quantum Electronics 53 (2021): 1-15.

[16] Upender, P., and Amarjit Kumar. "Quad-band circularly polarized tunable graphene based dielectric resonator antenna for terahertz applications." Silicon (2021): 1-14.

[17] Xue, Fan, et al. "Ultra-high sensitive refractive index sensor based on D-shaped photonic crystal fiber with graphene-coated Ag-grating." Heliyon 9.4 (2023).

[18] Kaur, Baljinder, Santosh Kumar, and Brajesh Kumar Kaushik. "Advances in photonic crystal fiber: sensing and supercontinuum generation applications." Optical Fiber Technology 72 (2022): 102982.

[19] Wang, Yujun, JianPing Shen, and Shuguang Li. "Surface plasmon induced broadband single-polarization filter based on high birefringence photonic crystal fiber." Optik 206 (2020): 164255.

[20] Cheng, Xu, et al. "Sandwiched graphene/hBN/graphene photonic crystal fibers with high electro-optical modulation depth and speed." Nanoscale 12.27 (2020): 14472-14478.

[21] Wang, Jianshuai, et al. "Wavelength-Switchable Polarization Filter Based on Graphene-Coated D-Shaped Photonic Crystal Fiber." Plasmonics 19.5 (2024): 2363-2370.